

## Vibration and Damping Behavior of Si<sub>3</sub>N<sub>4</sub> Reinforced Magnesium Alloy Composite for Structural Applications

C.K. Dhinakarraj<sup>1</sup>, N. Senthilkumar<sup>1,\*</sup>, M.A. Badri<sup>2</sup> and G. Anbuechhiyan<sup>3</sup>

<sup>1</sup> Adhiparasakthi Engineering College, Melmaruvathur, TamilNadu 603319, India

<sup>2</sup> BrahMos Aerospace Private limited, Hyderabad, Telangana 500058, India

<sup>3</sup> SRM Valliammai Engineering College, Kattangulathur, TamilNadu 603203, India

Corresponding Author Email: [nskmfng@gmail.com](mailto:nskmfng@gmail.com)

### ABSTRACT

For a variety of application, materials are demanded with high damping that can lower fundamental natural frequencies, and composites offer widespread options towards designing space structure with lightweight which are controlled effectively. Damping fixtures were made with lightweight composites, for the purpose of transporting aerospace components from one place to another. This present work investigates the damping characteristics of lightweight magnesium-based composite (AZ31+x%Si<sub>3</sub>N<sub>4</sub>), subjected to vibration. The composite cantilever beam is excited using an impact hammer and the vibrations generated are recorded using a data acquisition system. The damping properties are related to the density and microstructure of the fabricated composites. Results show that the damping factor changes with higher reinforcement of Si<sub>3</sub>N<sub>4</sub> ceramic particulates and the microstructure obtained during casting have an influence on the damping performance.

**Keywords:** magnesium composite, damping factor, microstructure, density, vibration

Received: June-10-2020, Accepted: July-17-2020, <https://doi.org/10.14447/jnmes.v23i3.a05>

### 1. INTRODUCTION

The method of transportation and logistics cycle of any consists of a series of risks such as integrity of load including vibrations. By measuring the parameters, vibrations can be characterized which allows engineers and researchers to simulate the real-time damages triggered by movement over the design of the package and to develop optimal packing that can protect the component against the threat of vibration [1]. A predominant method applied for detecting, monitoring, and analyzing the condition of a structure in real-time condition or over a period of time is vibration analysis performed through rapid data collection and data interpretation. Vibrations in structural components are hazardous for heavy machinery and equipment, and also for facilities, employees, and business consequential [2].

In the present scenario of modern transportation, noises and chatter produced is a health hazard for human beings [3], apart from that, uncontrolled vibration will lead to fatigue failure of machinery [4]. To avoid the adverse effect of vibration, materials are selected based on good damping properties, so as to absorb vibrations. For this, magnesium and their composites were a good choice, as they are light in weight with required mechanical properties and better damping characteristics. Presently in aerospace applications, fixtures made up of magnesium alloys are used for holding the aviation components during transit, in order to absorb the generated vibrations. Meanwhile, to strengthen the magnesium alloys, reinforcements are added to the base alloy to improve their

properties to the required condition without deteriorating their damping qualities.

Hoksbergen et al. [5] compared the vibration and damping characteristics of carbon fiber reinforced plastic (CRPF) with magnesium plates and identified that CFRP damping is higher than magnesium plates. As compared with magnesium plates the natural frequency of thin CFRP plates is almost the same. But the natural frequency of thicker CFRP sheets is lower than that of the magnesium sheets. Shunmugasamy et al. [6] examined the damping properties of various lightweight materials including magnesium and found that, with nanocomposites, damping capabilities tend to change which attributed to an increase in dislocation density, the thermal mismatch between filler and matrix, and grain boundary slide. Chung [7] identified that improvement in damping characteristics is mostly attributed to the microstructural design of metals, interface design for polymers, and the use of admixture for composite. Due to their viscoelasticity, metals and polymers tend to be better for damping than composite.

Zhang [8] concluded that pure magnesium matrix composites exhibit better tensile strength than pure magnesium and damping capacity is significantly reduced with an increase of reinforcement due to the movement of composite dislocations. Luo et al. [9] conducted damping loss factor testing and sound transmission experiments on AZ31B magnesium alloy with micro-arc oxidation coating and electrophoretic deposition process, an improvement in the frequency range of the damping loss factor from 0–850 Hz was observed and improvement in bending stress improves losses in sound transmission. Parande et al. [10] synthesized

eggshell particles reinforced in Mg-Zn and analyzed the damping performance of composite; damping capacities tend to improve monotonically as compared with Mg-2.5Zn-7ES composite, showing an improvement of nearly 105.2 percent compared with the Mg-2.5Zn alloy.

Yu et al. [11] investigated alloying elements influence in a solid solution of binary magnesium alloys through damping and mechanical properties investigation. The alloys yield strength and independent strain-amplitude related damping are mainly associated with the lattice distortion. The distortion of the lattice of Mg-1%Sn alloy is lowest and with alloy Mg-1% Zn producing higher distortion. Yu et al. [12] investigated the damping capacities AZ91D composite reinforced with titanium aluminium carbide particles and identified that damping capacity increases with increase with reinforcement because of high dislocation density. Srikanth et al. [13] fabricated SiC-reinforced magnesium composite and analyzed its vibration and damping characteristics and found that pure magnesium matrix damping was increased with the inclusion of ceramic SiC particles. Higher frequency of vibration causes a lower capacity of damping of Mg-SiC composite and monolithic magnesium specimens.

Hao et al. [14] performed damping studies on copper particles reinforced in magnesium AZ91 alloy and attained improved capacity in damping behavior when compared with unreinforced alloy. An increase in damping behavior is associated with dislocation Mechanism involved in increasing the damping capacity can be understood in terms of the dislocation initiation and move towards the interfaces due to variation in thermal shrinkage of matrix and strengthening. Somekawa et al. [15] investigated the shift in two-way mobility caused by twin-boundary segregation in pure magnesium with magnesium alloys and determined the damping characteristics before and after the heat-treated alloys through annealing. Binary magnesium alloy shows poor damping characteristics with pure magnesium, alloying elements of a magnesium alloy having low energy segregation characteristic for twin boundaries, effectively prevents degradation of the damping capacity.

Previous works related to the improvement of damping qualities revealed that the addition of reinforcement particles increases the mechanical properties and the damping factor values. Hence, from literature studies, the research gap is identified as least work was performed with AZ31 based ceramic reinforced composites in understanding their damping behavior for applications in aerospace engineering. Hence, an attempt is made to fabricate a novel  $\text{Si}_3\text{N}_4$  ceramic reinforced AZ31 based MMCs and to characterize it for their mechanical properties such as tensile strength, porosity, hardness, and impact strength as per ASTM standards and damping property in natural frequency using the cantilever beam method, which is the novelty and prime objective of this present study.

## 2. MATERIAL SELECTION AND EXPERIMENTAL PROCEDURES

The matrix material selected to fabricate the novel MMCs is AZ31 magnesium alloy, which contains magnesium (97%), aluminium (2.75%), zinc (0.9%) as major constituents and manganese (0.2%), silicon (0.1%), copper (0.05%), calcium (0.04%), iron (0.005%) and nickel (0.005%) as minor

constituents. It has a density of  $1.77 \text{ g/cm}^3$ . AZ31 is less dense than steel and aluminium and hence it is light in weight [16, 17].  $\text{Si}_3\text{N}_4$  is a ceramic, which possesses a density of  $2.37 \text{ g/cm}^3$  and tensile strength of 60 MPa and compressive strength of 524 MPa and also has very high resistivity to corrosion of acids and alkaline.  $\text{Si}_3\text{N}_4$  possess higher oxidation resistance, good fracture toughness, creep resistance, resistance to thermal shock, resistance to wear, and fatigue strength [18, 19].

The disintegrated melt deposition (DMD) method of liquid casting is adopted for fabricating the composite. For the fabrication of composite, one of the most widely adopted liquid casting technique is DMD. Through DMD, uniform distribution and dispersion of reinforcements are achieved which significantly increases the overall performance of the fabricated composites. Magnesium alloy is fed into the crucible and heated around  $800^\circ\text{C}$  and the preheated  $\text{Si}_3\text{N}_4$  ( $400^\circ\text{C}$ ) is added slowly and stirred well for 10 min with 500 rpm. The molten composite is then exited through the bottom on to a die placed in an argon atmosphere for obtaining a higher rate of solidification and to avoid oxidation and burning.  $\text{Si}_3\text{N}_4$  is added in different proportions (0, 2, 4, 6, 8, and 10% by wt.) in the matrix of AZ31 [20, 21]. The experimental methodology followed for completing the objectives is shown in Figure 1.

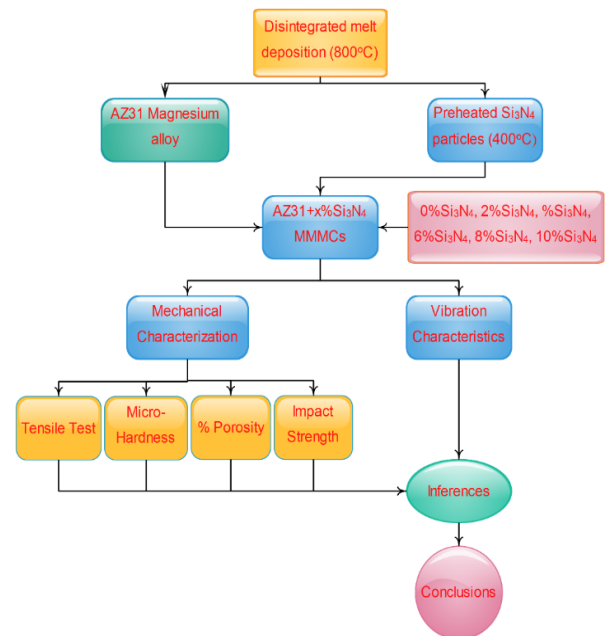


Figure 1. Experimental methodology

Mechanical properties; tensile strength is determined as per ASTM B557M standard [22], Vickers micro-hardness is determined as per ASTM E384-17 [23] and impact strength is determined in guideline with ASTM E23-07A [24]. The percentage of porosity is determined through the difference arising among the theoretical and experimental densities [25, 26]. The density of fabricated specimens is determined based on the Archimedes principle. The porosity of each composite is calculated according to Eq. (1).

$$Porosity = 1 - \left( \frac{\rho_a}{\rho_t} \right) \quad (1)$$

where  $\rho_t$  is the theoretic density and  $\rho_a$  is the actual density.

Vibration analysis comprises of transducer that is sensitive to vibration and equipment for measuring and recording the characteristics of vibration of the fabricated composites [27]. The vibration data is collected through a data acquisition system and is compared for all the fabricated composites [28]. For vibration analysis, the size of the workpiece considered is 70mmx40mmx15mm (LxBxT), which is fixed and considered as a cantilever beam as illustrated in Figure 2. An impact hammer is used to strike the cantilever beam (specimen of MMC) and the vibration is taken by the accelerometer attached with it, whose signal is given to a signal conditioner and subsequently to the signal analyzer and the amplitude of vibration is displayed in the monitor for analysis and interpretation.

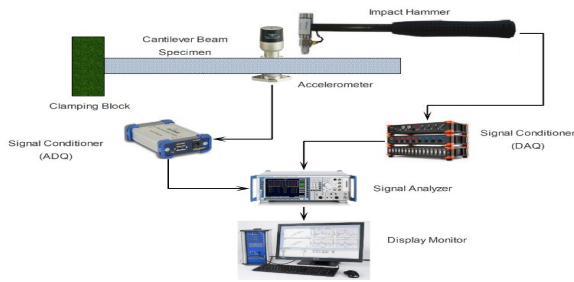


**Figure 2.** Illustration of cantilever beam setup for vibration analysis

The experimental setup is illustrated in Figure 2, the impact points are evenly selected on the specimens. The response pickup is obtained by acceleration transducer (model KISTLER 8776A50, Acceleration range:  $\pm 50g$ , Sensitivity: 100mV/g) for every impact by a force transducer (model KISTLER 9712B50, Acceleration range:  $\pm 50g$ , Sensitivity: 100mV/g). The signals are processed by DEWE 43 A.

### 3. RESULTS AND DISCUSSIONS

#### 3.1 Metallographic structure of fabricated MMCs

The SEM images of the as-cast and  $\text{Si}_3\text{N}_4$  reinforced AZ31 MMCs are presented in Figure 3. It is observed that a porous free structure was observed with even distribution of ceramic particulates [29, 30]. Higher ceramic particulates are visible in specimens reinforced with higher wt.% of ceramics in the matrix of AZ31. Formation of  $\text{Mg}_2\text{Si}$ ,  $\text{Mg}_3\text{N}_2$ , and  $\text{Mg}_{17}\text{Al}_{12}$  interphases along with  $\text{MgO}$  are found in the SEM images, due to the pseudo-eutectic transformation during the process of solidification in an inert atmosphere, which is the strengthening mechanism in MMCs.

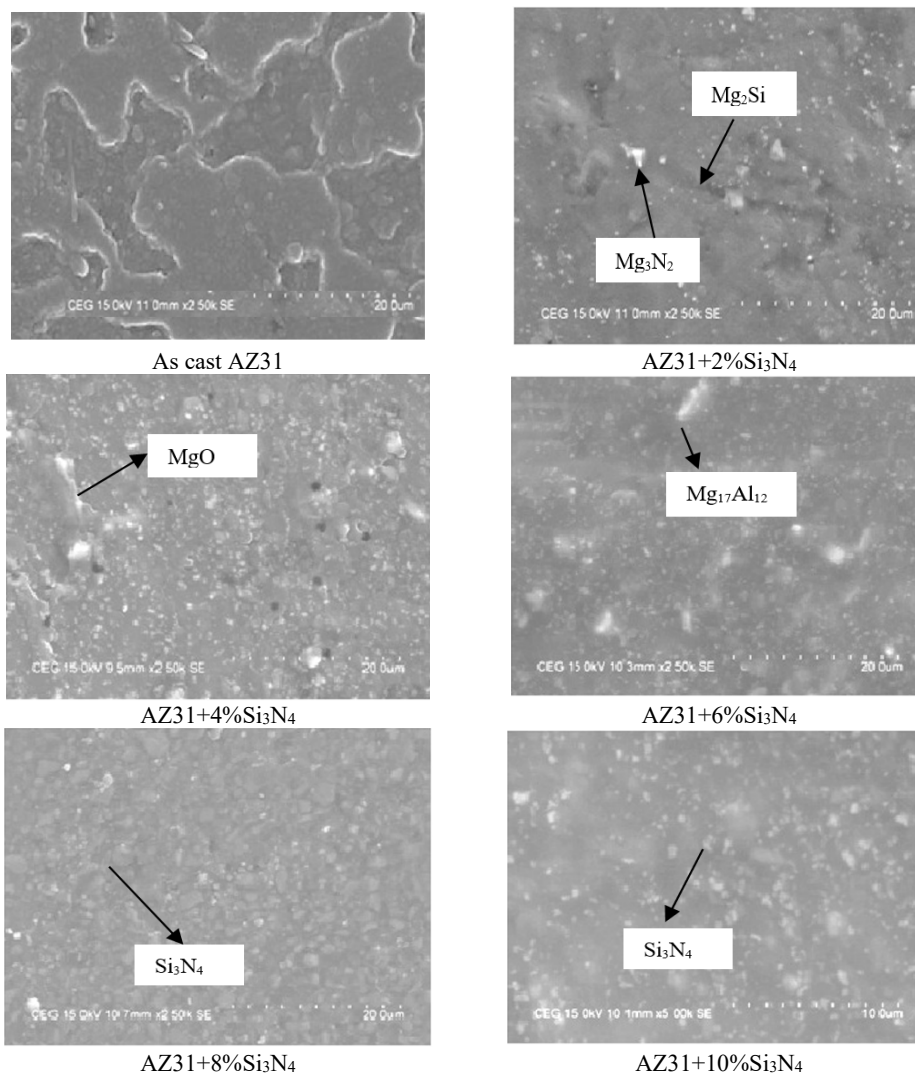


**Figure 3.** SEM images of as cast and magnesium composites

### 3.2 Mechanical characterization of fabricated MMCs

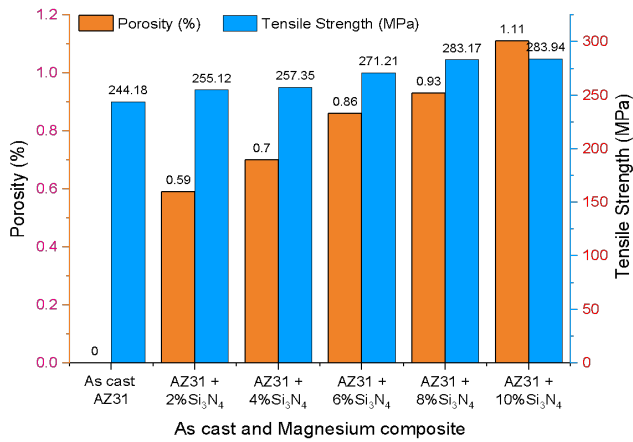


Figure 4. % porosity and tensile strength of fabricated materials

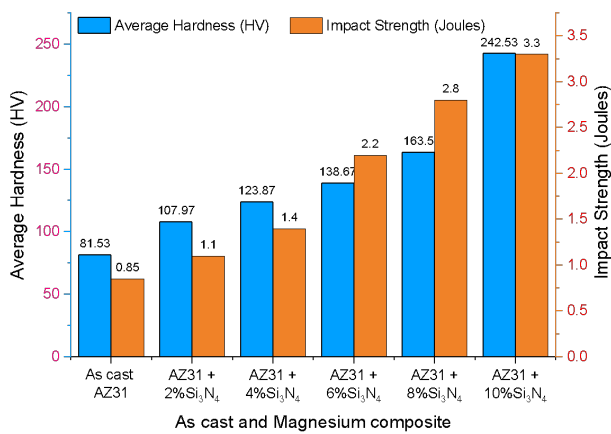


Figure 5. Vickers hardness and impact strength of fabricated materials

The fabricated MMCs were characterized by their mechanical properties. Figure 4 presents the influence of Si<sub>3</sub>N<sub>4</sub> addition on % porosity and tensile strength of various MMCs. Observation reveals that % porosity of the fabricated composites tends to increase with increasing wt.% of Si<sub>3</sub>N<sub>4</sub> in the matrix of AZ31, which is attributed to the

difference in thermal conductivities of the matrix and reinforcing phases and due to the oxidation nature of Si<sub>3</sub>N<sub>4</sub>. There was an increase in porosity from 0.59 to 1.11% due to the evolution of nitrogen and the presence of silicon porosity. An increase in the tensile strength is due to the toughness property of Si<sub>3</sub>N<sub>4</sub>, which takes the applied load and then evenly distributes it to the matrix material. The dislocation movement was blocked due to the precipitation of Mg<sub>2</sub>Si interphases and the presence of Si<sub>3</sub>N<sub>4</sub> on the boundaries of the grain and due to the Orowan strengthening mechanism (resists the dislocations to move further due to closely spaced hard ceramics).

The average micro-Vickers hardness of the fabricated MMCs and their impact strength are shown in Figure 5. Micro-Vickers hardness tends to increase with higher reinforcement of hard Si<sub>3</sub>N<sub>4</sub> particles, which resists the applied load during the test. The amalgamation of Si<sub>3</sub>N<sub>4</sub> particulate in the matrix increases the surface area and subsequently the hardness and impact strength. With increasing hardness, higher energy can be absorbed by the fabricated MMCs due to their ability to withstand impact load applied due to the incorporation of hard ceramic particles. With higher Si<sub>3</sub>N<sub>4</sub> incorporation, ductility tends to lower, but due to the high toughness, impact strength tends to improve.

### 3.3 Vibration and damping characterization

The fabricated composite materials are subjected to vibration analysis and with the usage of the frequency response function, the natural frequency of MMCs is determined. In the modal analysis, frequency response function (FRF), is a frequency-based function of measurement [31], used for identifying the modal shapes, damping characteristics, and resonant frequencies of a physical component/structure. FRF consists of both phase and amplitude and is a complex function. The response of FRF is generally a normalized value of the input, the peak frequency representing the FRF is the test specimens resonant frequencies [32]. Figure 6 to Figure 10 shows the FRG spectrum of fabricated MMCs using a bode plot (frequency vs displacement plot), showing the resonant frequency of the MMCs. From the graph output results, an increase in reinforcement material increases the resonant frequency because of the increase in mechanical properties. This allows lesser deflection because of stiffness.

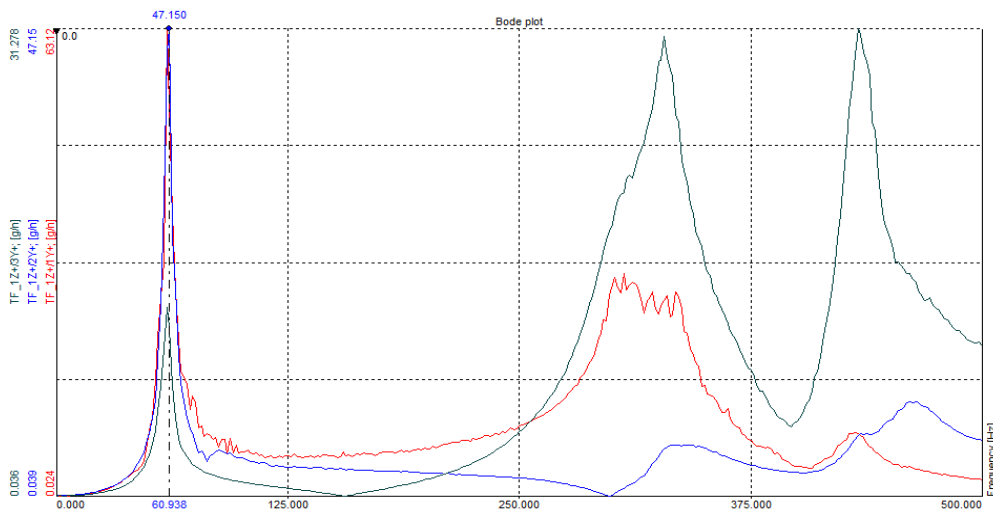


Figure 6. FRF spectrum of AZ31+2%Si<sub>3</sub>N<sub>4</sub> MMC

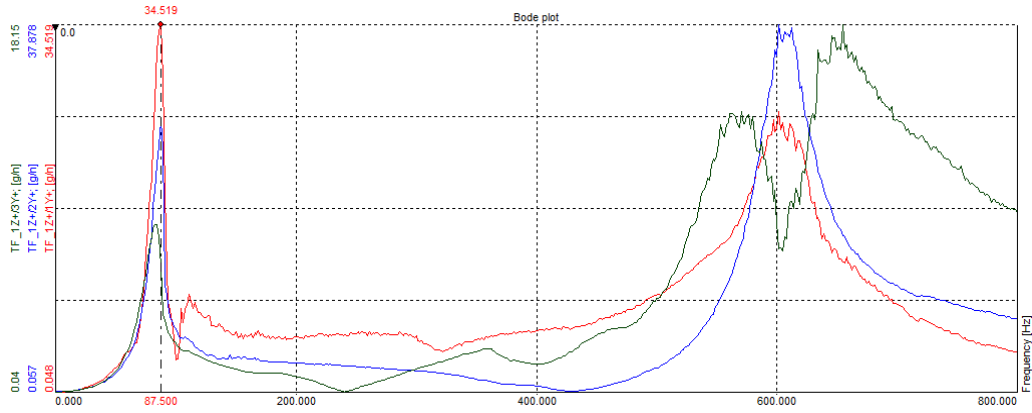


Figure 7. FRF spectrum of AZ31+4%Si<sub>3</sub>N<sub>4</sub> MMC

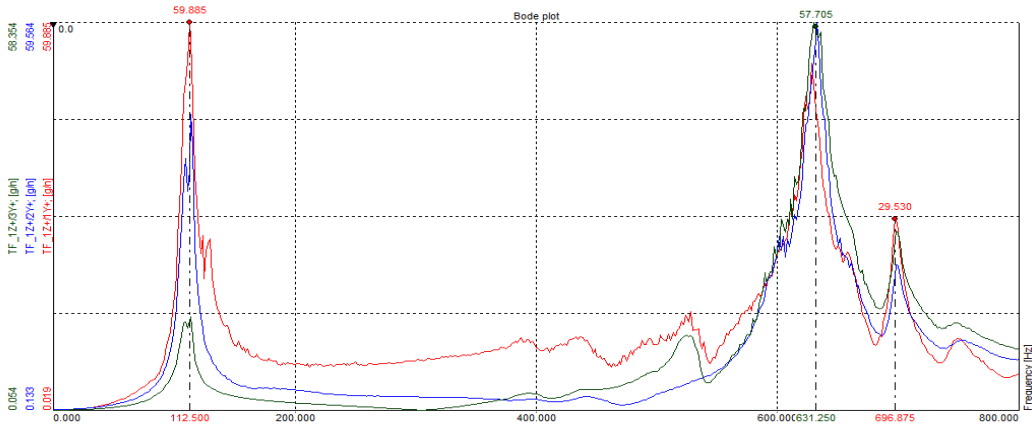


Figure 8. FRF spectrum of AZ31+6%Si<sub>3</sub>N<sub>4</sub> MMC

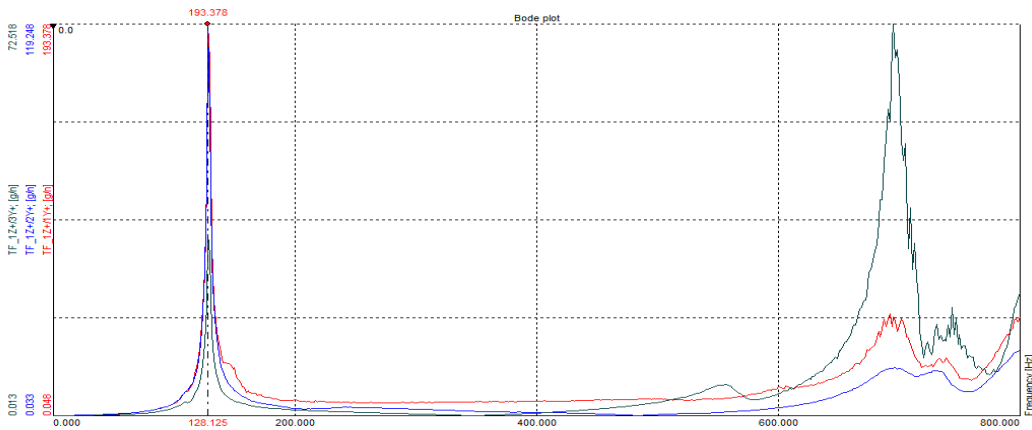


Figure 9. FRF spectrum of AZ31+8%Si<sub>3</sub>N<sub>4</sub> MMC

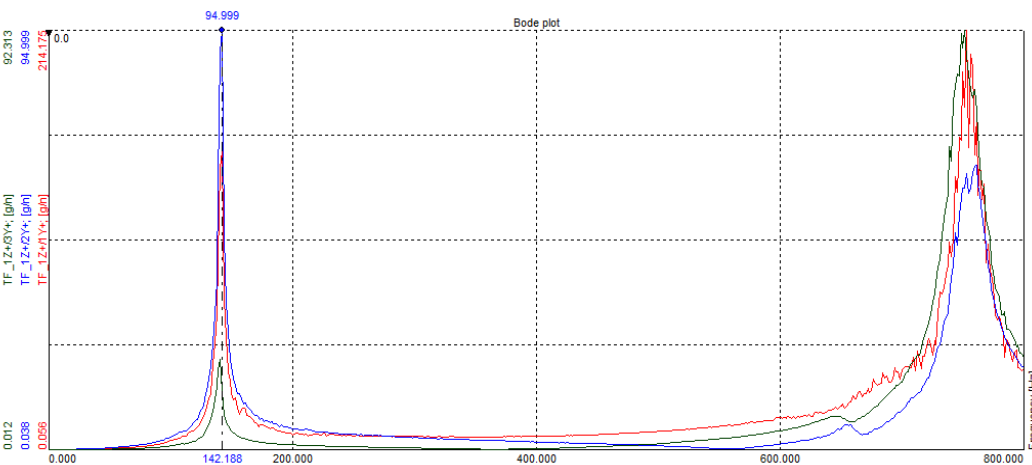


Figure 10. FRF spectrum of AZ31+10%Si<sub>3</sub>N<sub>4</sub> MMC

The circle fit of modal was used to find resonance and frequency damping estimation.

$$\eta = \frac{1}{Q} = 2\zeta = \frac{\%Cr}{50} = \tan \phi = \frac{\Delta\omega_{3dB}}{\omega_0} \quad (2)$$

where  $\eta$  = loss factor,  $Q$  = damping factor or quality factor,  $\zeta$  = Damping ratio,  $\%Cr$  = Percent of critical damping ( $\%Cr = 100\% \times \zeta$ ) and  $\phi$  = Phase angle between cyclic stress and strain. The damping factor  $Q$  of the model relates to the ratio of the frequency of resonant peak to the difference between the frequency 3 dB down from the peak value:

$$Q = \frac{f_0}{f_2 - f_1} = \frac{\omega_0}{\Delta\omega_{3dB}} \quad (3)$$

where  $f_0$  = peak resonant frequency (Hz),  $f_1$  = 3 dB lower frequency from peak frequency (Hz) and  $f_2$  = 3 dB lower peak frequency and  $>f_0$ . The Eq. (2) and (3) shows the relationship between damping characteristic and frequency of the model. Figure 11 shows the Nyquist plot of frequency response for all the fabricated MMMCs. From the graph of circular fit, the increase in the reinforcement reduces the damping of the composite [33, 34].

The graphs of the vibrational behavior of composites samples give the details of the resonant frequency damping factor, calculated by using the Eq. (3). The experimental findings of natural frequency, Quality factor, and loss factor are displayed in Figure 12 and Figure 13.

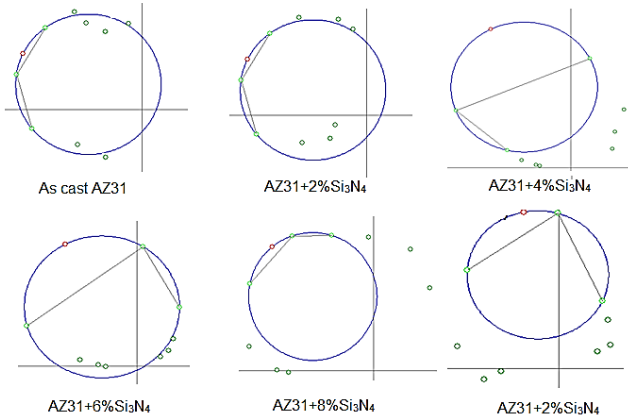


Figure 11. Nyquist plot of frequency response

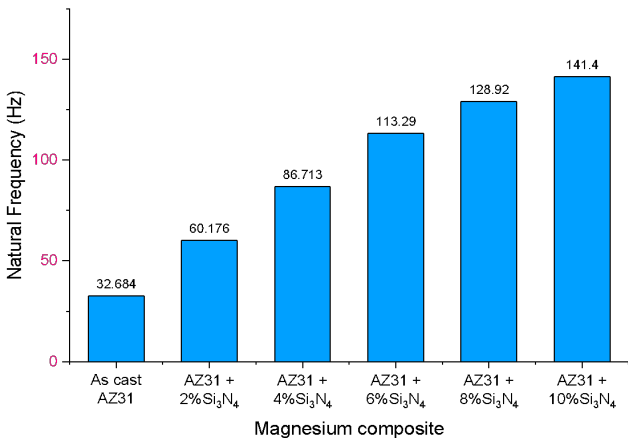


Figure 12. Natural frequencies of various MMMCs

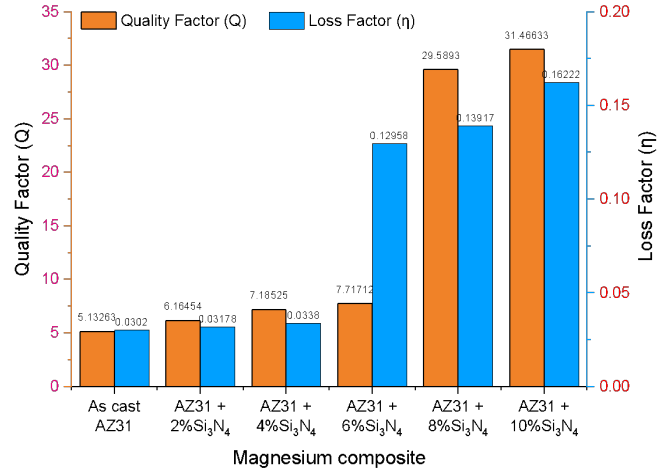


Figure 13. Quality and Loss factor obtained from analysis

From the graph, the increase in reinforcement increases the natural frequency of the composite. Figure 13 gives the understanding that the increase in quality factor and loss factor in connection with an increase in reinforcement also the damping ratio decreases with an increase in the reinforcement of the composite.

From the above result, the increase in reinforcement material increases the resonant frequency because of the increase in mechanical properties which allow lesser deflection because of the stiffness.

### 3.4 Simulation studies

In real-time engineering applications, engineering materials with specific properties are applied. In this work, for fixture application that requires good damping and mechanical properties is identified as, magnesium composite with high reinforcement (AZ31+10%Si<sub>3</sub>N<sub>4</sub>). Numerical simulation of vibration behavior of the MMMC is performed in ABAQUS simulation software using subspace Eigen solver. A 3D model of the workpiece is created (Figure 14) and the properties are defined. C3D20: A 20-node quadratic brick is used to mesh the workpiece model block [35, 36]. The mesh convergence study was used to check the mesh refinement. The simulated workpiece is provided in Figure 14.

The displacement is noted and data are noted the natural frequency is calculated by using the Eq. (4).

$$f_n = \frac{1}{2\pi} \sqrt{\frac{g}{\delta}} \quad (4)$$

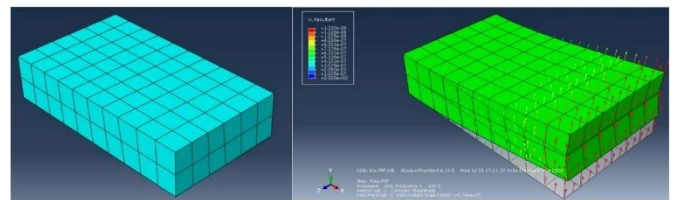


Figure 14. Modelling and simulation of AZ31+10%Si<sub>3</sub>N<sub>4</sub> MMMC

The natural frequency is calculated for simulation data and the graph is drawn as shown in Figure 15. The experimental natural frequency for AZ31+10% Si<sub>3</sub>N<sub>4</sub> is 141.4Hz, from

numerical simulation it is obtained as 140 Hz, the resonant frequency is nearly very similar to the experimental frequency. The simulation result gives evidence of the prepared material satisfies the mechanical properties and vibration characteristics.

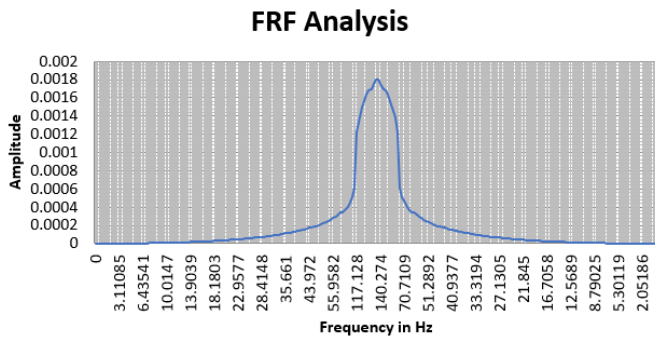


Figure 15. FRF Response curve

#### 4. CONCLUSIONS

A novel  $\text{Si}_3\text{N}_4$  reinforced AZ31 based MMCs were fabricated using the DMD method in an inert atmosphere and the fabricated composites were characterized for its mechanical, metallurgical, and vibration damping properties. The inferences made from the investigations are:

(1) Even distribution of ceramic particles is observed, with the formation of  $\text{Mg}_2\text{Si}$ ,  $\text{Mg}_3\text{N}_2$  interphases which improve the mechanical properties.

(2) The microhardness of the composites was increased from 107.9 VHN to 242.53 VHN due to the addition of hard  $\text{Si}_3\text{N}_4$  particulate. (i.e. from 2% to 10%).

(3) The addition of tough  $\text{Si}_3\text{N}_4$  particulate with more weight% as reinforcement has improved the tensile strength of composite from 255.12 MPa to 283.94 MPa and also increases the energy-absorbing capacity from 0.85J to 3.3J.

(4) The resonant frequency increases with an increase in reinforcement and the simulated result matches with the experimental result.

#### REFERENCES

- [1] Xu, Y.L., Xia, Y. (2011). Structural health monitoring of long-span suspension bridges. CRC Press.
- [2] Houser, D.R., Drosjack, M.J. (1973). Vibration signal analysis techniques. Ohio State Univ Columbus Dept Of Mechanical and Aerospace Engineering.
- [3] Berglund, B., Lindvall, T. (1995). Community noise. Stockholm: Center for Sensory Research, Stockholm University and Karolinska Institute.
- [4] Ellyin, F. (2012). Fatigue damage, crack growth and life prediction. Springer Science & Business Media.
- [5] Hoksbergen, J.S., Ramulu, M., Reinhall, P., Briggs, T.M. (2009). A Comparison of the vibration characteristics of carbon fiber reinforced plastic plates with those of magnesium plates. *Applied Composite Materials*, 16(5): 263-283. <https://doi.org/10.1007/s10443-009-9093-7>
- [6] Shunmugasamy, V.C., Mansoor, B., Gupta, N. (2016). Cellular magnesium matrix foam composites for mechanical damping applications. *Journal of the Minerals, Metals and Materials Society*, 68(1): 279-287. <https://doi.org/10.1007/s11837-015-1680-5>
- [7] Chung, D.D. (2003). Composite materials for vibration damping. In *Composite Materials*, Springer, London. 245-252.
- [8] Zhang, X.N. (2003). Effect of reinforcements on damping capacity of pure magnesium. *Journal of materials science letters*, 22(7): 503-505. <https://doi.org/10.1023/A:1022978117819>
- [9] Luo, Z., Hao, Z.Y., Jiang, B.L., Ge, Y.F., Zheng, X. (2014). Micro arc oxidation and electrophoretic deposition effect on damping and sound transmission characteristics of AZ31B magnesium alloy. *Journal of Central South University*, 21(9): 3419-3425. <https://doi.org/10.1007/s11771-014-2317-5>
- [10] Parande, G., Manakari, V., Koppa, S.D.S., Gupta, M. (2020). A study on the effect of low-cost eggshell reinforcement on the immersion, damping and mechanical properties of magnesium–zinc alloy. *Composites Part B: Engineering*, 182: 107650. <https://doi.org/10.1016/j.compositesb.2019.107650>
- [11] Yu, L., Yan, H., Chen, J., Xia, W., Su, B., Song, M. (2020). Effects of solid solution elements on damping capacities of binary magnesium alloys. *Materials Science and Engineering: A*, 772: 138707. <https://doi.org/10.1016/j.msea.2019.138707>
- [12] Yu, W., Li, X., Vallet, M., Tian, L. (2019). High temperature damping behavior and dynamic Young's modulus of magnesium matrix composite reinforced by  $\text{Ti}_2\text{AlC}$  MAX phase particles. *Mechanics of Materials*, 129: 246-253. <https://doi.org/10.1016/j.mechmat.2018.12.001>
- [13] Srikanth, N., Saravananathan, D., Gupta, M. (2004). Effect of presence of SiC and operating frequency on the damping behaviour of pure magnesium. *Materials science and technology*, 20(11): 1389-1396. <https://doi.org/10.1179/026708304225022269>
- [14] Hao, G.L., Han, F.S., Wu, J., Wang, X.F. (2007). Damping properties of porous AZ91 magnesium alloy reinforced with copper particles. *Materials science and technology*, 23(4): 492-496. <https://doi.org/10.1179/174328407X185758>
- [15] Somekawa, H., Basha, D.A., Singh, A., Tsuru, T., Watanabe, H. (2020). Change in damping capacity arising from twin-boundary segregation in solid-solution magnesium alloys. *Philosophical Magazine Letters*, 1-12. <https://doi.org/10.1080/09500839.2020.1805132>
- [16] Wang, Z., Guan, Y., Wang, T., Zhang, Q., Wei, X., Fang, X., Gao, S. (2019). Microstructure and mechanical properties of AZ31 magnesium alloy sheets processed by constrained groove pressing. *Materials Science and Engineering: A*, 745: 450-459. <https://doi.org/10.1016/j.msea.2019.01.006>
- [17] Wu, Y., Liu, J., Deng, B., Ye, T., Li, Q., Zhou, X., Zhang, H. (2020). Microstructure, Texture and Mechanical Properties of AZ31 Magnesium Alloy Fabricated by High Strain Rate Biaxial Forging. *Materials*, 13(14): 3050. <https://doi.org/10.3390/ma13143050>
- [18] Li, X., Yao, D., Zuo, K., Xia, Y., Yin, J., Liang, H., Zeng, Y.P. (2019). Fabrication, microstructural characterization and gas permeability behavior of porous silicon nitride ceramics with controllable pore structures. *Journal of the European Ceramic Society*, 39(9): 2855-

2861.  
<https://doi.org/10.1016/j.jeurceramsoc.2019.03.011>
- [19] Haubner, R., Herrmann, M., Lux, B., Petzow, G., Weissenbacher, R., Wilhelm, M. (2003). High performance non-oxide ceramics II, 102: Springer.
- [20] Hassan, S.F., Gupta, M. (2002). Development of a novel magnesium-copper based composite with improved mechanical properties. *Materials research bulletin*, 37(2): 377-389. [https://doi.org/10.1016/S0025-5408\(01\)00772-3](https://doi.org/10.1016/S0025-5408(01)00772-3)
- [21] Matli, P.R., Sheng, J.G.Y., Parande, G., Manakari, V., Chua, B.W., Wong, S.C.K., Gupta, M. (2020). A New Method to Lightweight Magnesium Using Syntactic Composite Core. *Applied Sciences*, 10(14): 4773. <https://doi.org/10.3390/app10144773>
- [22] Tian, S., Wang, L., Sohn, K. Y., Kim, K.H., Xu, Y., Hu, Z. (2006). Microstructure evolution and deformation features of AZ31 Mg-alloy during creep. *Materials Science and Engineering: A*, 415(1-2): 309-316. <https://doi.org/10.1016/j.msea.2005.10.015>
- [23] Caicedo, J.C., Quiñonez, S., Aperador, W. (2019). Mechanical and Tribological Analysis of Anodized AZ31 Magnesium Alloy as a Function of a Cement Concrete Environment. *Tribology in Industry*, 41(4): 563-572.
- [24] Verma, J., Taiwade, R.V., Reddy, C., Khatirkar, R.K. (2018). Effect of friction stir welding process parameters on Mg-AZ31B/Al-AA6061 joints. *Materials and Manufacturing Processes*, 33(3): 308-314. <https://doi.org/10.1080/10426914.2017.1291957>
- [25] Alam, M.E., Han, S., Nguyen, Q.B., Hamouda, A.M.S., Gupta, M. (2011). Development of new magnesium-based alloys and their nanocomposites. *Journal of Alloys and Compounds*, 509(34): 8522-8529. <https://doi.org/10.1016/j.jallcom.2011.06.020>
- [26] Pc, E., Radhakrishnan, G., Emarose, S. (2020). Investigation into Physical, Microstructural and Mechanical Behaviour of Titanium dioxide Nanoparticulate Reinforced Magnesium Composite. *Materials Technology*, 1-10. <https://doi.org/10.1080/10667857.2020.1782050>
- [27] Rao, S.S. (2005). *Mechanical Vibrations (SI Edition)*. [28] Weaver Jr, W., Timoshenko, S.P., Young, D.H. (1990). *Vibration problems in engineering*. John Wiley & Sons.
- [29] Abbas, A., Huang, S.J., Ballóková, B., Sülleiová, K. (2020). Tribological effects of carbon nanotubes on magnesium alloy AZ31 and analyzing aging effects on CNTs/AZ31 composites fabricated by stir casting process. *Tribology International*, 142: 105982. <https://doi.org/10.1016/j.triboint.2019.105982>
- [30] Ceschini, L., Dahle, A., Gupta, M., Jarfors, A.E.W., Jayalakshmi, S., Morri, A., Singh, R.A. (2017). *Aluminum and magnesium metal matrix nanocomposites*. Springer.
- [31] Hassan, S.F., Gupta, M. (2005). Enhancing physical and mechanical properties of Mg using nanosized  $\text{Al}_2\text{O}_3$  particulates as reinforcement. *Metallurgical and Materials Transactions A*, 36(8): 2253-2258. <https://doi.org/10.1007/s11661-005-0344-4>
- [32] Srikanth, N., Lim, C.V., Gupta, M. (2000). The modeling and determination of dynamic elastic modulus of magnesium based metal matrix composites. *Journal of Materials Science*, 35(18): 4661-4666. <https://doi.org/10.1023/A:1004886503104>
- [33] Srikanth, N., Gupta, M. (2002). Damping characterization of Mg-SiC composites using an integrated suspended beam method and new circle-fit approach. *Materials Research Bulletin*, 37(6): 1149-1162. [https://doi.org/10.1016/S0025-5408\(02\)00735-3](https://doi.org/10.1016/S0025-5408(02)00735-3)
- [34] Srikanth, N., Gupta, M. (2003). Damping characterization of magnesium based composites using an innovative circle-fit approach. *Composites science and technology*, 63(3-4): 559-568. [https://doi.org/10.1016/S0266-3538\(02\)00231-2](https://doi.org/10.1016/S0266-3538(02)00231-2)
- [35] Cao, D.X., Wang, J.J., Gao, Y.H., Zhang, W. (2019). Free Vibration of Variable Width Beam: Asymptotic Analysis with FEM Simulation and Experiment Confirmation. *Journal of Vibration Engineering & Technologies*, 7(3): 235-240. <https://doi.org/10.1007/s42417-019-00116-1>
- [36] Biswas, P., Mandal, D., Mondal, M.K. (2020). Failures analysis of in-situ Al-Mg<sub>2</sub>Si composites using actual microstructure-based model. *Materials Science and Engineering: A*, 140155. <https://doi.org/10.1016/j.msea.2020.140155>